

© Copyright 1993 American Meteorological Society (AMS). Permission to use figures, tables, and brief excerpts from this work in scientific and educational works is hereby granted provided that the source is acknowledged. Any use of material in this work that is determined to be “fair use” under Section 107 of the U.S. Copyright Act or that satisfies the conditions specified in Section 108 of the U.S. Copyright Act (17 USC §108, as revised by P.L. 94-553) does not require the AMS’s permission. Republication, systematic reproduction, posting in electronic form on servers, or other uses of this material, except as exempted by the above statement, requires written permission or a license from the AMS. Additional details are provided in the AMS CopyrightPolicy, available on the AMS Web site located at (<http://www.ametsoc.org/AMS>) or from the AMS at 617-227-2425 or [copyright@ametsoc.org](mailto:copyright@ametsoc.org).

Permission to place a copy of this work on this server has been provided by the AMS. The AMS does not guarantee that the copy provided here is an accurate copy of the published work.

## ANOMALOUS PROPAGATION ASSOCIATED WITH THUNDERSTORM OUTFLOWS

Mark E. Weber, Melvin L. Stone and Joseph A. Cullen  
MIT/Lincoln Lab Lexington, Massachusetts

## 1. INTRODUCTION

Battan [1] noted that ducting of radar energy by anomalous atmospheric refractive index profiles and resulting abnormally strong ground clutter can occur during three types of meteorological circumstance: (i) large scale boundary layer temperature inversions and associated sharp decrease in moisture with height — these are often created by nocturnal radiative cooling; (ii) warm, dry air moving over cooler bodies of water, resulting in cooling and moistening of air in the lowest levels; (iii) cool, moist outflows from thunderclouds.

In contrast to the first two types of anomalous propagation (AP), radar ducting associated with thunderstorm outflows is quite dynamic and may mimic echoes from precipitating clouds in terms of spatial scale and temporal evolution. While non-coherent weather radars (e.g. WSR-57) are obviously susceptible to false storm indications from this phenomenon, Doppler radars that select the level of ground clutter suppression based on "clear day maps" may also fail to suppress the AP-induced ground clutter echoes. Operational Doppler radar systems known to be susceptible to this phenomena are the National Weather Service's WSR-88D (Sirmans, personal communication) and the Federal Aviation Administration's Airport Surveillance Radar (ASR-9) six-level weather channel [2].

In this paper, characteristics of thunderstorm outflow-generated AP are documented using data from a testbed ASR-9 operated at Orlando, Florida. The testbed radar's rapid temporal update (4.8 seconds per PPI scan) and accurate scan-to-scan registration of radar resolution cells enabled characterization of the spatial and temporal evolution of the AP-induced clutter echoes. We discuss implications of these phenomenological characteristics on operational systems, specifically the ASR-9. Algorithms for discrimination between true precipitation echoes and AP-induced ground clutter are discussed.

## 2. AP MEASUREMENTS WITH ASR-9

The ASR-9 testbed in Orlando, Florida [3] operated at 2.8 GHz, transmitting a 1 MW, 1  $\mu$ s uncoded pulse at an average PRF of 1100 per second. The antenna's half-power beamwidth is 1.4° in azimuth and approxi-

mately 5° in elevation; the tilt of the antenna places the peak of the elevation pattern 2° above the horizon and the lower half-power point on the horizon. In-phase and quadrature signals are sampled at intervals of 0.775  $\mu$ s and simultaneously stored on high density instrumentation tape and processed to generate real-time displays of precipitation reflectivity, mean Doppler and spectrum width. Small-scale divergent outflows (microbursts) and outflow boundaries (gust fronts) are detected by automated algorithms, displayed and tracked in real time. The instrumented range for the algorithms extends 30 km from the radar; maps of weather spectrum moments are generated to a range of 111 km.

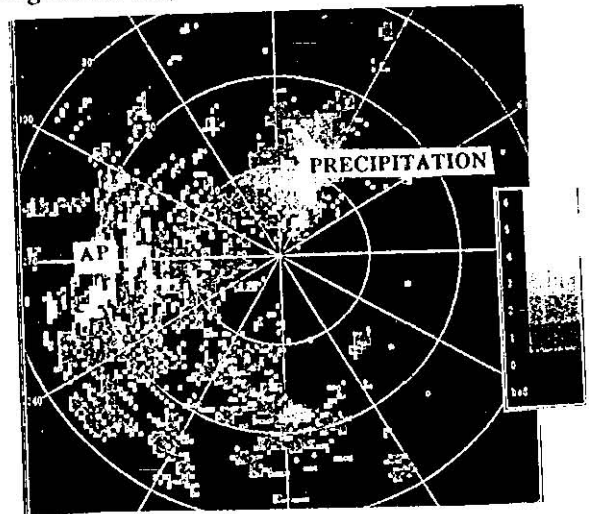


Figure 1. PPI scan of reflectivity (quantized in NWS "VIP" units) during an AP-episode. Range rings at 10 km intervals.

Data from six separate occurrences of thunderstorm-generated AP during the months of August and September 1991 and 1992 were examined for this paper. Significant enhancement of ground clutter during these episodes was observed at ranges up to 50 nmi — the strongest returns exceeded 65 dBz equivalent reflectivity factor and the largest AP area observed was about 200 square kilometers. Duration of the significant AP-induced ground clutter episodes varied from 1.25 to more than 2.5 hours. During these episodes, individual "patches" — closed regions containing echoes in excess of 35 dBz equivalent reflectivity — varied in duration from a few minutes to the lifespan of

the AP episode. Figure 1 shows a reflectivity map generated by the ASR-9 testbed during one of these episodes. Normal ground clutter has been removed by highpass filters, selected using a "clear day map" [4]; the remaining echoes are precipitation and AP-induced ground clutter; the latter echoes are primarily to the south and west of the radar at ranges greater than 15 km. Note that some of the AP echoes to the west are contiguous to or even embedded in 20 to 35 dBz precipitation echoes to the west of the radar.

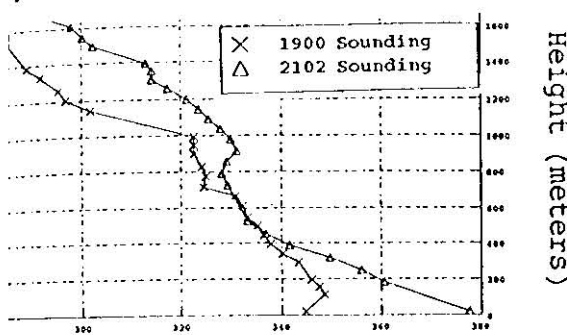


Figure 2. Radar refractivity ("N units") profile derived from pre- and post-gust front rawinsonde soundings.

Each AP episode occurred following the passage of a thunderstorm outflow boundary (gust front) over the radar site. In the above example, a strong, eastward-moving gust front passed over the ASR-9 about 30 minutes prior to the depicted scan. Pre- and post-gust front rawinsonde soundings showed significant cooling and moistening in the lowest 500 meters; maximum changes in temperature and dew point were at the surface and equalled 6 and 3 °C respectively. The resulting increase in radio refractivity gradient below 500 m is shown in Figure 2. The AP areas are observed only in the sector behind the gust front, implying that the superrefractive environment must be maintained along the entire path between the radar and the ground scatterers responsible for the echoes.

In general, the patches of strong AP-induced ground clutter appear suddenly (when the outflow boundary has passed 5–10 km beyond the radar), remain approximately constant in intensity and spatial extent for a period of time, then dissipate rapidly over the entire affected area. A characteristic time scale for onset or dissipation of individual AP patches is 5 to 10 minutes. During the constant phase of the AP episode, echo intensity variation in time is small, consistent with scan-to-scan fluctuations in normal ground clutter cross-section [4]. Specific geographic areas are con-

sistent sources of strong echoes with repeatable spatial reflectivity patterns.

Figure 3 compares power spectrum estimates from AP-induced ground clutter breakthrough and stratiform precipitation. Spectra of the AP-induced echoes are indistinguishable from normal clutter, consisting of a zero mean Gaussian component with spectrum width (0.75 m/s) consistent with antenna scan modulation. Precipitation echoes as sensed by the fan-beam ASR-9 — even the low mean Doppler stratiform rain echo shown in Figure 3 — consistently exhibit significantly larger spectrum width owing to vertical shear in the horizontal wind.

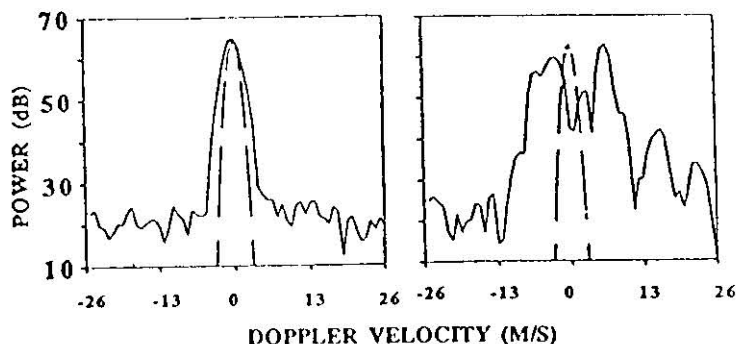


Figure 3. Power spectrum estimates of AP-induced clutter (left) and stratiform precipitation (right). Dashed lines show theoretical antenna scan-modulation spectrum.

### 3. AP-Induced Ground Clutter Rejection

Use of a high-pass ground clutter filter in all range-azimuth resolution cells would eliminate stationary clutter breakthrough caused by AP. Such filtering may not be desirable, however, since low-Doppler power removed by the filters may result in biases in weather reflectivity or mean Doppler estimates. This effect is exacerbated in the case of the rapid-scanning ASR-9, since the available coherent processing intervals are short (8 or 10 pulses) and the transition bands associated with achievable high-pass filters are large [4].

The ASR-9 weather channel and the WSR-88D attempt to minimize these biases by utilizing site-specific clear day maps of normal ground clutter to select the minimum level of clutter suppression necessary to achieve acceptable weather signal to clutter ratios. With this scheme, a "censoring" function should be introduced to identify stationary ground clutter breakthrough caused by abnormal propagation conditions.

Data from affected resolution cells are flagged and can be either disregarded in subsequent processing, or reprocessed using a more attenuating high-pass filter so as to suppress the clutter component of the echo.

We have examined two algorithms for discriminating between AP ground clutter breakthrough and actual precipitation echoes; both depend on the differing spectral characteristics of AP and precipitation echoes. Direct calculations of echo spectrum moments were utilized by an ASR-9 Wind Shear Processor [3] to censor AP-induced clutter breakthrough. The censor flag was set for range-azimuth resolution cells where the mean Doppler velocity was less than 1 m/s and the echo spectrum width was less than 1.5 m/s. Spatial consensus filters were applied to the censor flags (e.g. M-of-N filters along the range axis or 2-dimensional median filters) to remove "speckle" associated with weather moment estimate errors, particularly in the lower intensity AP areas. Figure 4 illustrates the effect of this censoring process using the scan shown previously. The censoring process largely removes the AP without significant impact on the precipitation echoes. The capability to remove AP echoes from the ASR-9's six-level reflectivity display was favorably received by the Orlando Air Traffic Control team during operational testing of the Wind Shear Processor in 1991 and 1992.

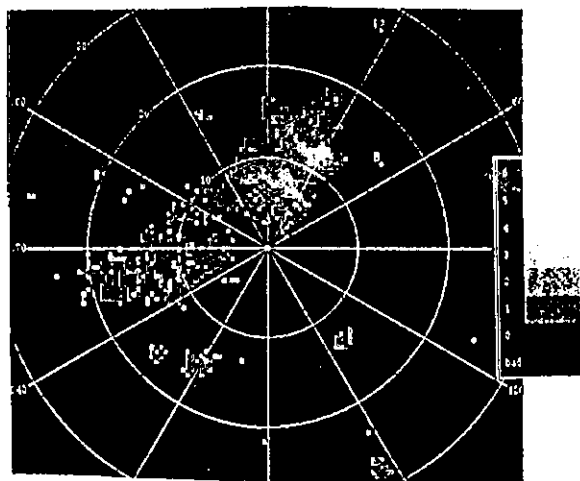


Figure 4. As in Figure 1 but with AP-discriminant enabled.

An alternate approach [2] exploits the "inverse matched filter" characteristics of the high-pass ground clutter filters. AP-induced clutter echoes will be subject to large attenuation when passed through these filters; attenuation of weather echoes with higher mean Doppler and spectrum width is much smaller. A power threshold test applied to the ratio of clutter

filter input and output can effectively discriminate between AP-induced clutter breakthrough and precipitation. Details and performance examples are provided in [2].

The above techniques appear sufficient for Air Traffic Control applications where some errors in the exact intensity and areal extent of precipitation echoes are tolerable. Improved performance, useful for example in hydrological applications, may be obtainable by augmenting these single-gate spectral discriminants with "expert system" knowledge on the characteristics of AP-induced echoes and the likelihood of superrefraction. Elements of such a system would include measurements of the spatial statistics of the echoes, surface temperature and humidity measurements — potentially augmented by a refractometer, reliable automated detection of outflow boundaries [5] and knowledge of the locations of ground scatterers likely to be illuminated during AP. The site specific information necessary for this last element may be obtained by means of detailed terrain maps and appropriate propagation models, or experimentally through accumulation of statistics on scattering regions from many AP episodes.

#### 4. Summary

Anomalous propagation, while well documented since early work on radar meteorology, remains an operational problem — particularly when it occurs in association with thunderstorm activity. This paper discussed spatial, temporal and spectral properties of AP-induced ground echoes associated with surface outflows from thunderclouds. We used data from a testbed ASR-9 to demonstrate a reliable spectral discriminant between AP-induced ground echoes and actual precipitation returns. In combination with additional sources of information relevant to the onset of AP, we believe that performance sufficient to support automated hydrological monitoring in the presence of this interferer can also be achieved.

#### REFERENCES

1. L. Battan, *Radar Observations of the Atmosphere*, University of Chicago Press, 1959.
2. D. Pazzo, S. Troxel, M. Meister, M. Weber, J. Pieronek, ASR-9 Weather Channel Test Report, Lincoln Laboratory Report ATC-165, DOT-FAA-PS-89-3, 1989.
3. M. Weber, M. Stone, C. Primm, J. Anderson, Airport Surveillance Radar Based Wind Shear Detection, Preprint Volume: Fourth International Conference on Aviation Weather Systems, June 24-28, 1991, Paris, France, AMS.
4. M. Weber, Ground Clutter Processing for Wind Measurements with Airport Surveillance Radars, Lincoln Laboratory Report ATC-143, DOT-FAA-PM-87-21, 1987.
5. R. Delany and S. Troxel, A Machine Intelligent Gust Front Algorithm for Doppler Weather Radars, Preprint Volume: 26th International Conference on Radar Meteorology, 24-28 May, 1993, Norman, OK., AMS.